

8-27-2025

Accurate Skin Lesion Segmentation through Feature Fusion in Dermoscopy Images

Fallah H. Najjar

Department of Emergent Computing, Faculty of Computing, Universiti Teknologi Malaysia, Johor Bahru, 81310, Malaysia AND Department of Computer Networks and Software Techniques, Technical Institute of Najaf, Al-Furat Al-Awsat Technical University, Najaf, 54001, Iraq, fallahnajjar@atu.edu.iq

Farhan Mohamed

Department of Emergent Computing, Faculty of Computing, Universiti Teknologi Malaysia, Johor Bahru, 81310, Malaysia, farhan@utm.my

Asniyani Nur Haidar Abdullah

Department of Emergent Computing, Faculty of Computing, Universiti Teknologi Malaysia, Johor Bahru, 81310, Malaysia AND Faculty of Information & Communication Technology, Universiti Teknikal Malaysia Melaka Hang Tuah Jaya, 76100 Durian Tunggal, Melaka, Malaysia, asniyani@utem.edu.my

Mohd Shafry Mohd Rahim

Department of Emergent Computing, Faculty of Computing, Universiti Teknologi Malaysia, Johor Bahru, 81310, Malaysia, shafry@utm.my

Karrar A. Kadhim

Department of Emergent Computing, Faculty of Computing, Universiti Teknologi Malaysia, Johor Bahru, 81310, Malaysia AND Computer Techniques Engineering Department, Faculty of Information Technology, Imam Ja'afar Al-Sadiq University, Baghdad, Iraq, karrar.zahid@gmail.com
Follow this and additional works at: <https://bsj.uobaghdad.edu.iq/home>

How to Cite this Article

Najjar, Fallah H.; Mohamed, Farhan; Abdullah, Asniyani Nur Haidar; Rahim, Mohd Shafry Mohd; and Kadhim, Karrar A. (2025) "Accurate Skin Lesion Segmentation through Feature Fusion in Dermoscopy Images," *Baghdad Science Journal*: Vol. 22: Iss. 8, Article 30.
DOI: <https://doi.org/10.21123/2411-7986.5041>

This Article is brought to you for free and open access by Baghdad Science Journal. It has been accepted for inclusion in Baghdad Science Journal by an authorized editor of Baghdad Science Journal.



RESEARCH ARTICLE

Accurate Skin Lesion Segmentation through Feature Fusion in Dermoscopy Images

Fallah H. Najjar^{1,2,*}, Farhan Mohamed^{1,*}, Asniyani Nur Haidar Abdullah^{1,3},
Mohd Shafry Mohd Rahim¹, Karrar A. Kadhim^{1,4}

¹ Department of Emergent Computing, Faculty of Computing, Universiti Teknologi Malaysia, Johor Bahru, 81310, Malaysia

² Department of Computer Networks and Software Techniques, Technical Institute of Najaf, Al-Furat Al-Awsat Technical University, Najaf, 54001, Iraq

³ Faculty of Information & Communication Technology, Universiti Teknikal Malaysia Melaka Hang Tuah Jaya, 76100 Durian Tunggal, Melaka, Malaysia

⁴ Computer Techniques Engineering Department, Faculty of Information Technology, Imam Ja'afar Al-Sadiq University, Baghdad, Iraq

ABSTRACT

In the diagnosis of skin cancer, dermoscopy images have to be evaluated for feature extraction. In this paper, the authors design a new method to enhance the skin dermoscopy image segmentation accuracy by eliminating artifacts and hair using photometric quasi-invariants, followed by a unique approach for skin lesion segmentation using histogram-based feature fusion. Histogram features are used to extract data range and mean images from the histogram, and these are fused with the free artifacts and hair image to generate the final image. The authors used the PH2 dataset for the proposed segmentation method because it contains the ground truth for each image. In contrast, they used the Skin_Hair dataset, which includes artificial hair generated with its corresponding ground truth. On the other hand, some PH2 dataset images have hair artifacts that the proposed pre-processing method can remove. According to the experimental results, our method outperforms existing methods in three aspects: accuracy, efficiency, and robustness, measured by Accuracy (Acc), Precision (Pre), Sensitivity (Sen), Specificity (Spe), Jaccard Index (JI), and Dice (D). Our proposed method achieved an average Acc 96.14, Pre 93.87, Sen 94.49, Spe 95.99, JI 88.19, and D 94.21. Furthermore, the Spe increases to 95.99%, up by about +3.2% over top performing methods. In the meanwhile, JI is brought to 88.19%, which increases by about 1.5%; D takes over and goes up to value of 94.21%. These findings suggest that our methodology can provide a more effective and accurate way of detecting skin cancer.

Keywords: Artifacts and hair removal, Dermoscopic, Feature fusion, Segmentation, Skin cancer

Introduction

Dermoscopy is a non-invasive method that dermatologists have increasingly used to assist in the early diagnosis and differential diagnosis of melanocytic lesions, providing greater detail of the lesions than is possible the sole visual inspection, which is difficult to establish a definitive diagnosis if it is solely based on visual aspects.¹ Dermoscopy has provided valuable assistance in the diagnosis of cutaneous lesions,

particularly in the early detection of melanoma, a threatening skin cancer.² Nevertheless, in practice, complex anatomic structures like hairs and artifacts frequently obscure critical diagnostic features in dermoscopic images, thus making it challenging for dermatologists to diagnose skin lesions accurately.³ However, hair artifacts in dermoscopic images may also disturb the automatic analysis of these images, thereby decreasing the reliability of Computer-Aided Diagnosis (CAD) systems. In contrast, the last few

Received 29 June 2024; revised 14 October 2024; accepted 16 October 2024.
Available online 27 August 2025

* Corresponding authors.

E-mail addresses: fallahnajjar@atu.edu.iq (F. H. Najjar), farhan@utm.my (F. Mohamed), asniyani@utem.edu.my (A. N. H. Abdullah), shafry@utm.my (M. S. M. Rahim), Karrar.zahid@gmail.com (K. A. Kadhim).

<https://doi.org/10.21123/2411-7986.5041>

2411-7986/© 2025 The Author(s). Published by College of Science for Women, University of Baghdad. This is an open-access article distributed under the terms of the Creative Commons Attribution 4.0 International License, which permits unrestricted use, distribution, and reproduction in any medium, provided the original work is properly cited.

years have mobilized the development of methods that mainly aim to remove hair artifacts from dermoscopic images. Hair artifacts may take on various shapes, textures, and sizes, which complicates the task of developing one global method to remove hair in most cases.⁴ Furthermore, in some situations, the removal of hair artifacts from dermoscopic images can lead to losing critical diagnostic features, and thereby, the removal needs to be balanced with the amount of diagnostic information to be preserved.⁵ In recent times, significant progress has been made in the research of hair artifact removal in dermoscopic images. New methods have been emerging to improve the effectiveness and efficiency of other methods.⁶ However, there is still scope for further improvement, and designing better techniques to remove hair artifacts from dermoscopic images is an active research area.^{7,8}

In addition, an important and challenging problem is hair artifact removal in dermoscopic images, which has been widely studied by the research community.⁹ Dermoscopy has been widely used in dermatology, and accurate hair artifact removal in dermoscopic images is vital in the field to assist dermatologists in the diagnosis of skin lesions and to improve the accuracy of computer-aided diagnosis systems.¹⁰ Medical image segmentation, on the other hand, is the process of segmenting an image into different regions with similar properties or features. In the case of skin dermoscopy, image segmentation, for example, consists of the separation of skin lesions from healthy skin areas. A good segmentation process of skin lesions¹¹ facilitates correct identification. Despite the advancements in skin lesion segmentation algorithms, several factors can still hinder the accurate detection of the lesion or its structures. For example, complex color variations, sensitivity to hair, artifacts, and low-contrast situations are common reasons the lesion may not be detected with precision.^{12,13} Furthermore, the presence of a complex background, indistinct or irregular borders, or other structures in the image can also cause false skin lesion detection, leading to a failure to identify its structures.^{3,14,15} This paper aims to precisely detect skin lesions in dermoscopic images, followed by an accurate diagnosis or prognosis of the identified lesions. The precise segmentation of skin lesions can significantly enhance the diagnosis and management of skin conditions and illnesses while providing insights into potential risk factors and guiding treatment decisions. In addition, this automated process can also alleviate the burden on healthcare professionals by performing some of the analysis tasks involved in scrutinizing medical images. Our main contributions in this study are: (i) The

authors present a method for artifacts and digital hair removal to eliminate the artifacts and hair in the images, making the segmentation process more effective. The photometric quasi-invariants are the image features invariant to photometric changes in the image. The proposed technique extracts these features from the image and uses them to remove artifacts and hair. Then, the extracted features are normalized using the Z-score normalization method to make them invariant to the image scale. (ii) The authors proposed a skin lesion segmentation methodology using histogram feature fusion. The proposed method extracts the histogram data range and mean images to help identify skin lesion areas accurately. However, this paper is organized as follows. Initially, a critical review of the relevant published works in the related field is conducted. Then, a description of the algorithms employed in the proposed approach is given. Following that, a comprehensive explanation of the design of the proposed scheme and its flexibility is provided. Afterward, the effectiveness of the proposed scheme is assessed, followed by an analysis of the obtained results. Finally, to conclude, the paper summarizes the main findings and contributions.

Related works

Recently, significant advances have been made in the pre-processing and segmentation of dermoscopic images. For example, Alenezi et al.¹⁶ proposed a denoise tool for the dermoscopic image, which does not remove any unnecessary hair. Their method is attractive because it improves the clarity of lesions by simplifying hair details and also enhances the lesion images. In their proposed pre-processing method, the authors first use a method based on max pooling (3×3) layers and normalization to eliminate hair details from dermoscopy images. Then, the authors used the dilation process with filters of different sizes, like 1×1 , 2×2 , and 3×3 , to clear the image of the lesion. This process aims to show some small details and remove noise in dermoscopy images for better classification results. Li et al.¹⁷ presented a deep learning approach to hair removal that outperforms pure segmentation methods for skin lesion images. Their methodology involves using a deep learning network to learn a hair mask from manually annotated images. Subsequently, the mask of hair is combined with the original image to abolish hair, resulting in a hairless skin lesion image. The authors detail the deep learning network's preparation of the training and test sets and implementation details. The proposed method was tested on a dataset of skin

lesion images according to several performance metrics. The authors conclude that by removing digital hairs, it is likely that skin lesion segmentation accuracy can be improved further.

Attia et al.¹⁸ developed a hair simulation method for generating realistic hair patterns in skin lesion images. The tool can be used to evaluate image analysis algorithms and operates with a Generative Adversarial Network (GAN) to simulate hair patterns in melanoma images. Its goal is to more accurately segment hair as well as the lesions themselves, to improve the performance of segmentation and classification algorithms. The paper not only introduces the hair simulation tool, but also describes how it is implemented and evaluates it compared to other hair simulation tools in skin lesion images. The results showed that this tool gave more realistic hair patterns than alternative ones, and it can be used as a benchmark for testing parallel hair detection algorithms. The researchers concluded that the hair simulator is likely to raise the overall accuracy of skin lesion diagnostic algorithms in practical situations troubled by hair. Goyal et al.¹⁹ introduced a method for accurately segmenting skin lesions in dermoscopic images with an ensemble of deep learning algorithms. The proposed method combines CNNs and ResNets to learn image spatial characteristics, extract image features and classify every pixel.

A Conditional Random Field (CRF) is then used to refine the segmentation map so as to improve the localization of boundaries further. The method was tested on publicly available dermoscopic image dataset and found to outperform current state-of-the-art (SOTA) methods in both accuracy and computational efficiency. According to the authors, the proposed method can be used as a tool in skin cancer detection as well, which would make it possible to increase both accuracy and efficiency over the current clinical workflow. In their method, Abhishek et al. aim to boost the performance of basic skin-lesion segmentation for dermoscopic images by adding transformations based on the intensity of illumination.²⁰ They transform the image into a color space that isolates achromatic and chromatic information. Then, within each of the chromatic channels, they use illumination-based transformations to enhance the contrast between the lesion and the surrounding skin. This processed image will be used for segmentation using a deep learning model. They put their approach to the test by experimenting on a dermoscopic image dataset, and compared with state-of-the-art methods, the finer-grained results were just better. The authors also suggest that this approach may form a pre-processing step in practical applications

to improve skin lesion segmentation rates. Xie et al. proposed a skin lesion segmentation algorithm using the High-Resolution CNN (HR-CNN).²¹ Their method was designed to deal with high-resolution images and can therefore learn more efficient extraction of multi-scale features for detecting skin lesions. The authors used a dermoscopic image dataset to test their own method against some other top-of-the-range state-of-the-art methods. HR-CNN outperformed every such means in terms of both total accuracy and amount spent on computation. The authors hold that their method could be a tool for diagnosing skin cancer and improving clinical practices.

Ramya et al.²² proposed a skin lesion image segmentation algorithm using the discrete wavelet transform (DWT). Having conducted a literature survey into skin lesion segmentation, the authors found that methods including thresholding, clustering, and deep learning are all limited by the effect of noise on results, dependence on expert knowledge, and dependence on data volume. Therefore, the authors suggest that the images, after undergoing preliminary treatment by DWT in order to remove noise and use contrast enhancement for pre-processing, then have conventional thresholding applied so as to produce a better chance at eliminating false positives incorporated into Otsu's technique. Their experimental results showed higher degrees of segmentation accuracy than other methods. Araújo et al.²³ formulated an AI model that combines transfer learning strategies and fine-tuning pre-trained deep neural networks (DNNs) in order to segment images of melanoma skin cancer lesions automatically. The work found that traditional methods for segmentation were generally good as far as the accuracy of the final diagnosis was concerned. However, to obtain high accuracy, complex handcrafted features must be used with any conventional method of segmentation. In contrast, although deep learning methods based on large, annotated databases produced better results, this required much annotated data as well as powerful computer hardware that is difficult for everyone to possess. The authors thus proposed that in order to perform transfer learning, a deep neural network pre-trained on a larger dataset would be re-trained and then adapted to the target dataset by reducing the amount of data used for training. In the end, their experiments showed that such a job is better than SOTA methods. It can be argued that transfer learning and fine-tuning are effective ways of managing the lack of ground-truth segmentation data.

Chen et al.²⁴ described RACNNs, which exploit Recurrent Attention (RA) mechanisms within CNNs

to achieve selective attention at certain parts of an image. Experimental results revealed that the proposed method surpasses several SOTA techniques in segmentation accuracy, with high sensitivity and specificity proving the RACNN method can effectively model rich spatial and contextual information for skin lesions. Zafer et al. presented a MCC method for skin lesion classification based on deep learning and feature selection with the Slime Mould Algorithm (SMA).²⁵ The authors suggested employing DeepLabv3+, a state-of-the-art deep learning model for image segmentation, to cut skin lesions out from photos and extract features. They employed SMA to select an optimal subset of features, leveraging the ability of this algorithm to solve optimization problems by the shortest path of evolution. The experimental results showed that the study outperformed SOTA methods in classification accuracy. In short, the results prove that a combination of deep learning and feature selection based on SMA is effective for skin lesion classification. Wang and his colleagues used curriculum learning to create the GRNet, a new kind of neural network architecture that gradually adds recurrent connections to the traditionally convolutional structure for 2D medical image segmentation.²⁶ They put forward a new curriculum learning method, where for training it is antediluvian, hopelessly simple images which the network must learn to segment step by step—slowly reaching habit complexity not only by increasing input image size but also with feedback loops in its structure and round after round of learning on the back-propagated output. Where the results of basic properties for repeated curve sliding, their segmentation strategy not only lags behind SOTA, but lags very far behind it. However, Table 1 displays a summary of the related discussed articles.

Materials and methods

The authors present a new mathematical process combining the golden rule with theoretical probability. Furthermore, the authors developed this technique after analyzing nine different categories of natural light variation and optical artifacts. In this manner, the reliability of image segmentation based on our method has been dramatically improved. Last but not least, it could cover the whole scope of medical image processing, from the detection and measurement of various diseases to surgical navigation, orthopedic planning, MRI, CT, and other imaging modalities. The pre-processing scheme in this paper is specially designed to solve the non-trivial structures, such as artifacts and hair removal in skin dermoscopy images, based on the photometric quasi-invariants theory around an exemplar image. The hair pixel scalar and multi-scale approach is used for estimating hair pixels, and a photometric quasi-invariant algorithm is used to remove hair while retaining the underlying skin texture. Quasi-invariants, or “photo quasi-invariants”, are expressions in terms of intensity values from the surrounding pixels. Therefore, the calculation of these quasi-invariants for each pixel in the picture allows pixels to be identified as untrustworthy or colored inaccurately.

Pre-processing stage

The first step in the pre-processing pipeline is to capture the variation in the Hue, Saturation, and Value (HSV). The results of the HSV derivatives at this stage can then be used to try to detect whether hair or noise is present. For a given color image $I(r, c)$ represented by its channels, Red (R), Green (G), and Blue (B), the HSV derivatives are computed as follows:

Table 1. Summary of the related works.

Author(s)	Method	Key Features
Alenezi et al. ¹⁶	Denoise tool for dermoscopic images.	Uses max pooling and dilation to remove noise and simplify hair details.
Li et al. ¹⁷	Deep learning approach to hair removal.	Learns a hair mask with a deep network and applies it to original images.
Attia et al. ¹⁸	Hair simulation with GAN.	Simulates realistic hair patterns for the evaluation of algorithms.
Goyal et al. ¹⁹	Ensemble deep learning for lesion segmentation.	Combines CNNs and ResNets, uses CRF for boundary refinement.
Abhishek et al. ²⁰	Illumination-based transformation for segmentation.	Enhances contrast in chromatic channels.
Xie et al. ²¹	HR-CNN for skin lesion segmentation.	Efficient multi-scale feature extraction.
Ramya et al. ²²	Discrete wavelets transform for image pre-processing.	Removes noise, enhances contrast, and uses thresholding.
Araújo et al. ²³	Transfer learning and fine-tuning for melanoma segmentation	Combines pre-trained DNNs with transfer learning.
Chen et al. ²⁴	RACNNs with Recurrent Attention mechanisms.	Selective attention within CNNs for richer spatial information.
Zafer et al. ²⁵	MCC method with Slime Mould Algorithm for feature selection.	Uses DeepLabv3+ for segmentation and SMA for feature optimization.
Wang et al. ²⁶	GRNet with curriculum learning.	Gradually increases image complexity and network connections.

Hue derivatives (h_x , h_y) are calculated to understand how the color hue changes across the image, which improves the identification of color variations that could indicate the presence of hair or other features using Eq. (1).

$$h_i = \frac{R \times (B_i - G_i) + G \times (R_i - B_i) + B \times (G_i - R_i)}{\varsigma} \quad (1)$$

Saturation derivatives (S_x , S_y) measure changes in the saturation level across the image, which can be investigated for variations in color intensity and purity using Eq. (2).

$$S_i = \frac{R \times (2 \times R_i - G_i - B_i) + G \times (2 \times G_i - R_i - B_i) + B \times (2 \times B_i - R_i - G_i)}{\sqrt{3} \times \varsigma} \quad (2)$$

Value Derivatives (v_x , v_y) are computed to detect changes in the intensity of the image using Eq. (3).

$$v_i = \frac{R_i + G_i + B_i}{\sqrt{3}} \quad (3)$$

Where ς represents the normalization of the hue and saturation derivatives. It represents the overall intensity of the image and can be calculated using Eq. (4):

$$\varsigma = 2 \times \sqrt{R^2 - G^2 - B^2 - R \times G - R \times B - G \times B + \varepsilon} \quad (4)$$

Where ε is a small constant added for numerical stability, in order to analyze changes in hue, saturation, and intensity, the Gaussian derivatives were applied to each RGB channel. Gaussian derivatives are essential in image processing for edge detection, feature extraction, and smoothing while preserving the boundaries and details of significant features. The Gaussian derivatives for a given channel of the input image are represented by Eq. (5).

$$R_i = \frac{i}{\sigma^2} \cdot G(i; \sigma) \quad (5)$$

Similarly, G_i and B_i follows the same pattern, and $G(i; \sigma)$ represents the Gaussian derivatives, which are defined using Eq. (6).

$$G(i; \sigma) = \frac{1}{\sqrt{2\pi}\sigma^2} \cdot e^{-\frac{i^2}{2\sigma^2}} \quad (6)$$

Where σ represents the standard deviation and i represents the spatial coordinate x and y . Next, a combined spatial derivatives magnitude A is calculated to detect areas with potential noise or significant texture changes. This magnitude is calculated using Eq. (7):

$$A = \sqrt{h_x^2 + h_y^2 + S_x^2 + S_y^2 + v_x^2 + v_y^2 + \varepsilon} \quad (7)$$

After that, the binary mask BW is created by thresholding A . Pixels with a magnitude greater than a threshold τ (e.g., 15) are marked as 1 (true), indicating potential noise or edges. The BW is created by using Eq. (8).

$$BW = \{1 \text{ if } A > \tau \text{ } 0 \text{ if } A \leq \tau \quad (8)$$

The binary mask is dilated using a disk-shaped structuring element z with a radius of 3 pixels. This operation can be represented as in Eq. (9):

$$BW1 = \text{dilation}(BW, z) \quad (9)$$

For each color channel C of the image $I(r, c)$, noise regions identified by the dilated mask $BW1$ are filled using the region fill function. This can be denoted as in Eq. (10):

$$I_C = \text{regionfill}(I_C, BW1) \quad (10)$$

The final, noise-reduced image Q is reconstructed by concatenating the filled channels as in Eq. (11):

$$Q = \text{cat}(3, I_R, I_G, I_B) \quad (11)$$

Segmentation stage

Although region filling is a valuable tool in medical imaging, its utility is restricted due to inherent limitations and challenges in handling complex structures. These errors include detail loss, boundary inaccuracies, overfilling, and underfilling. White balance and gamma correction techniques can mitigate these drawbacks by isolating infected regions from the background. To implement these techniques, the authors apply them to the hair-free image. White balance removes any color casts that resulted from using different light sources during image capture, while gamma correction increases the visibility of details and textures in the lesion. These techniques can help achieve higher accuracy and resolution in medical imaging, particularly for intricate structures.

The next step in our proposed method involves convolving the original image with a 3×3 mask to obtain

the first-order histogram probability. This probability is calculated by dividing the frequency of the pixel value by the total number of pixels in the mask (9 for a 3×3 mask) using Eq. (9). The symbol $GP(g)$ denotes the frequency of the pixel value at gray level g , while IP represents the total number of pixels in the mask²⁷ as in Eqs. (12) to (15).

$$P(g) = \frac{GP(g)}{IP} \quad (12)$$

The image (mean) is computed using the following equation.

$$I_{\mu}(g) = \sum_{g=1}^{IP} g P(g) \quad (13)$$

The image (data range) will be calculated using the following formula:

$$I_{DT} = (g) - (g) \quad (14)$$

The following formula fused the histogram features with the free hair and noise image.

$$FI(x, y) = I_F + I_{\mu}(g) + I_{DT} \quad (15)$$

This fusion process allowed the segmentation algorithm to leverage the additional information provided by the histogram features, resulting in more accurate and robust segmentation results. As a result, the technique is effective in various applications, including medical image analysis, object detection, and scene understanding, as shown in the experimental results section, see Fig. 1.

Results and discussion

These are the results of our approach, validated with an experimental section. Statistical findings are calculated in the pre-processing step over 252 dermoscopic images of the Skin_Hair dataset, while in the segmentation step, the same analysis is performed for 200 images in the PH2 dataset.

Experimental setup

The proposed approach was implemented using MATLAB R2022a on a Windows 11 operating system. Furthermore, the experiments were conducted on a computer with a 2.30 GHz Intel Core i7-11 CPU, 16 GB RAM, and 4 GB GPU.

Datasets

The authors conducted experiments on the Pedro Hispano Hospital (PH2) dataset containing 200 dermoscopic images with ground truth segmentation masks,²⁸ belonging to three types of lesions: atypical nevus, common nevus, and melanoma. In addition, six segmentation performance metrics were used to evaluate our proposed method. However, the PH2 dataset consisted of 200 images, each with its corresponding ground truth image.

The PH2 dataset is a publicly available dataset of dermoscopic images of pigmented skin lesions, which can be used for dermatology and CAD research on skin lesions. Additionally, the results of the experiment were conducted on the Skin_Hair dataset.¹⁵ The Skin_Hair dataset contains 252 dermoscopic images containing artificial hair. Check out Fig. 2, which

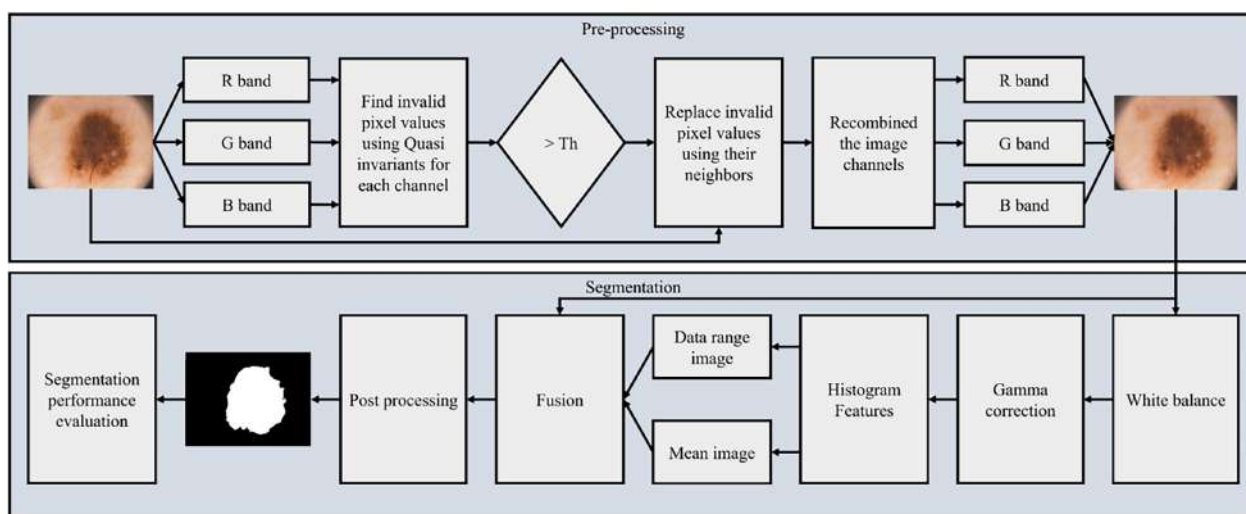


Fig. 1. Structure of the proposed technique.

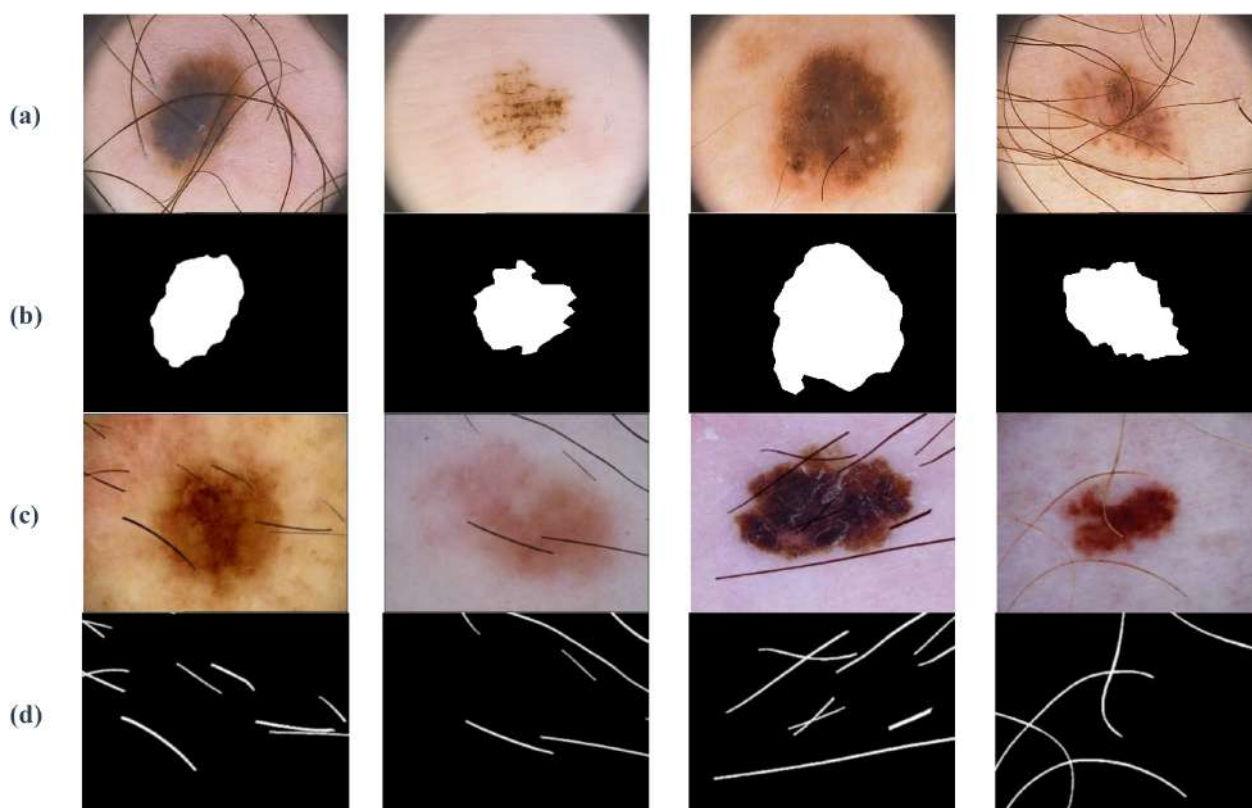


Fig. 2. Dataset image samples with the ground truth (a and b) Ph2²⁸ and (c and d) Skin_Hair¹⁵.

shows a selection of the PH2 dataset images analyzed in this study.

Image pre-processing results

In this study, the authors compare the proposed pre-processing method with the SOTA methods in terms of three image quality metrics: SSIM (Structural Similarity Index), PSNR (Peak Signal-to-Noise Ratio), and MSE (Mean Squared Error). These metrics are commonly used to assess pre-processed images' quality and determine how well the proposed method performs compared to SOTA methods.

However, the performance of the proposed pre-processing was experimented on the Skin_Hair dataset,¹⁵ since the Skin_Hair dataset has artificial generated hair for all images, while the PH2 dataset does not, see Fig. 2. Table 2 displays the comparison results of the proposed pre-processing method.

Table 2. Skin_Hair dataset pre-processing results (overall).

Method	SSIM	PSNR	MSE
Navier-Stokes ¹⁵	0.9590	40.3050	7.3800
Telea ¹⁵	0.9590	40.5580	7.1140
Hair SinGAN ¹⁵	0.8810	34.4890	53.735
R-Mnet ¹⁵	0.9600	40.6550	23.743
Our pre-processing	0.9785	40.5373	4.1898

From Table 2, it is clear that the proposed pre-processing method outperforms most of the SOTA methods in terms of SSIM and MSE while achieving comparable results in terms of PSNR. Specifically, the proposed pre-processing method achieves an SSIM score of 0.9785, significantly higher than all SOTA methods. These results indicate that the proposed method produces pre-processed images with significantly improved structural similarity compared to the other methods. Additionally, the proposed method achieves a shallow MSE score of 4.1898, significantly lower than all of the SOTA methods. Finally, the results demonstrate that the proposed method can produce pre-processed images very close to the original images, with minimal distortion.

Regarding PSNR, the proposed pre-processing method achieves a score of 40.5373, comparable to most of the SOTA methods listed in the table. In addition, while some SOTA methods achieve slightly higher PSNR scores, the difference is insignificant, indicating that the proposed method is competitive in this metric. Furthermore, Fig. 3 displays the proposed pre-processing results.

The impact of pre-processing

In order to assess its efficacy, the authors carried out tests with and without pre-processing procedures.

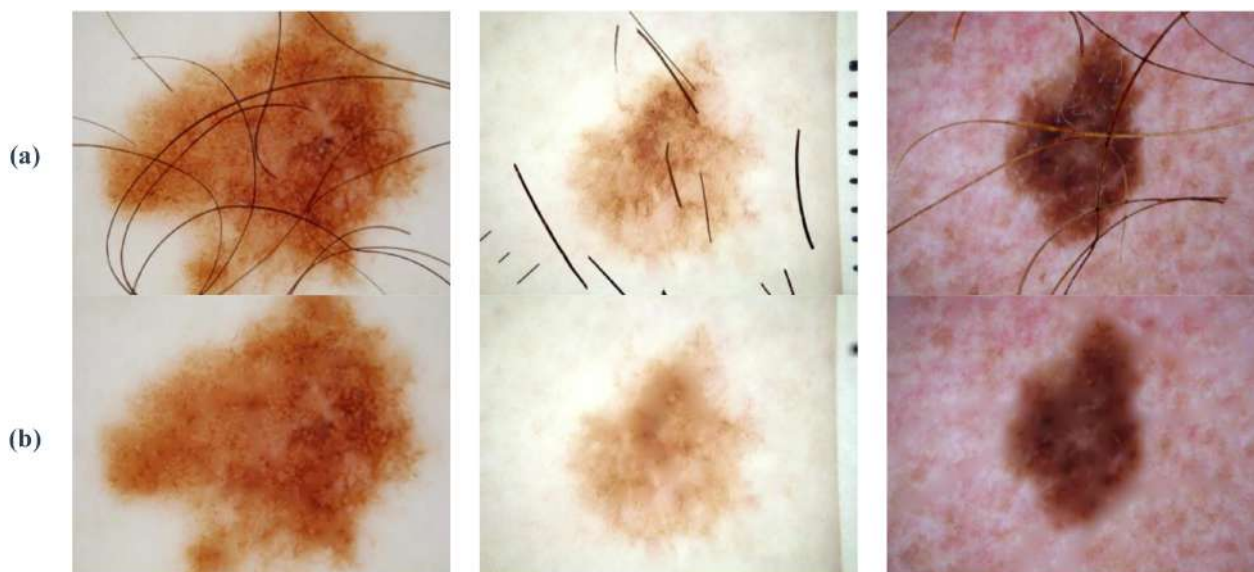


Fig. 3. Pre-processing results on the Skin_Hair dataset¹⁵ (a) original image and (b) pre-processed image.

Specifically, the authors applied our suggested segmentation technique with and without these steps and discovered that all metrics exhibited improvement by eliminating hair and enhancing contrast, as outlined in Table 3.

Table 3. PH2 dataset segmentation results (Mean \pm Standard Deviation) with (WP) and without (WOP) pre-processing.

Metric	WOP (%)	WP (%)
Acc	94.89 \pm 0.0651	96.14 \pm 0.0613
Pre	92.51 \pm 0.0902	93.87 \pm 0.0860
Sen	93.06 \pm 0.0798	94.49 \pm 0.0759
Spe	95.21 \pm 0.0877	95.99 \pm 0.0825
JI	86.19 \pm 0.0968	88.19 \pm 0.0968
D	92.25 \pm 0.0652	94.21 \pm 0.0649

Table 3 indicates that utilizing pre-processing enhances the performance of the segmentation technique. Specifically, when pre-processing is employed, all metrics exhibit better results than when not used. Moreover, the enhancements are consistent across all the metrics, with average values ranging from 1.25% to 2.00%. Both the JI and D measures are utilized to assess the segmentation performance by calculating the overlap between the segmented area and the ground truth. These metrics are considered reliable for evaluating segmentation performance. The study shows that pre-processing leads to a gain of approximately 2% in both the JI and D coefficient, which suggests that pre-processing is beneficial in accurately segmenting the skin lesion. The outcomes of this study demonstrate that our pre-processing method considerably improves the accuracy and robustness of the segmentation technique. Also, our proposed

pre-processing method was successfully applied to an existing skin lesion segmentation method,²⁰ demonstrating significant improvements over the baseline methods.

Table 4. PH2 dataset segmentation results with (WP) and without (WOP) pre-processing.

Abhishek et al. ²⁰		
Metric	WOP (%)	WP (%)
Acc	89.26	90.88
Sen	84.42	87.51
Spe	96.07	96.99
JI	75.59	78.14
D	85.37	87.57

Table 4 compares the skin lesion segmentation results before and after pre-processing. The results show that pre-processing improved the performance of skin lesion segmentation for all metrics. For example, the accuracy increased from 89.26% to 90.88%, sensitivity increased from 84.42% to 87.51%, and specificity increased from 96.07% to 96.99%. In addition, the JI and D improved significantly after pre-processing, indicating better overlap between the predicted and ground truth masks. For example, the JI increased from 75.59% to 78.14%, and the D increased from 85.37% to 87.57%. Our method effectively increased the accuracy of the segmentation process, resulting in more precise and reliable identification of skin lesions. Furthermore, the result confirms that the pre-processing steps augment the input images and elevate the quality of segmentation results. Furthermore, the pre-processing results are displayed in Fig. 4.

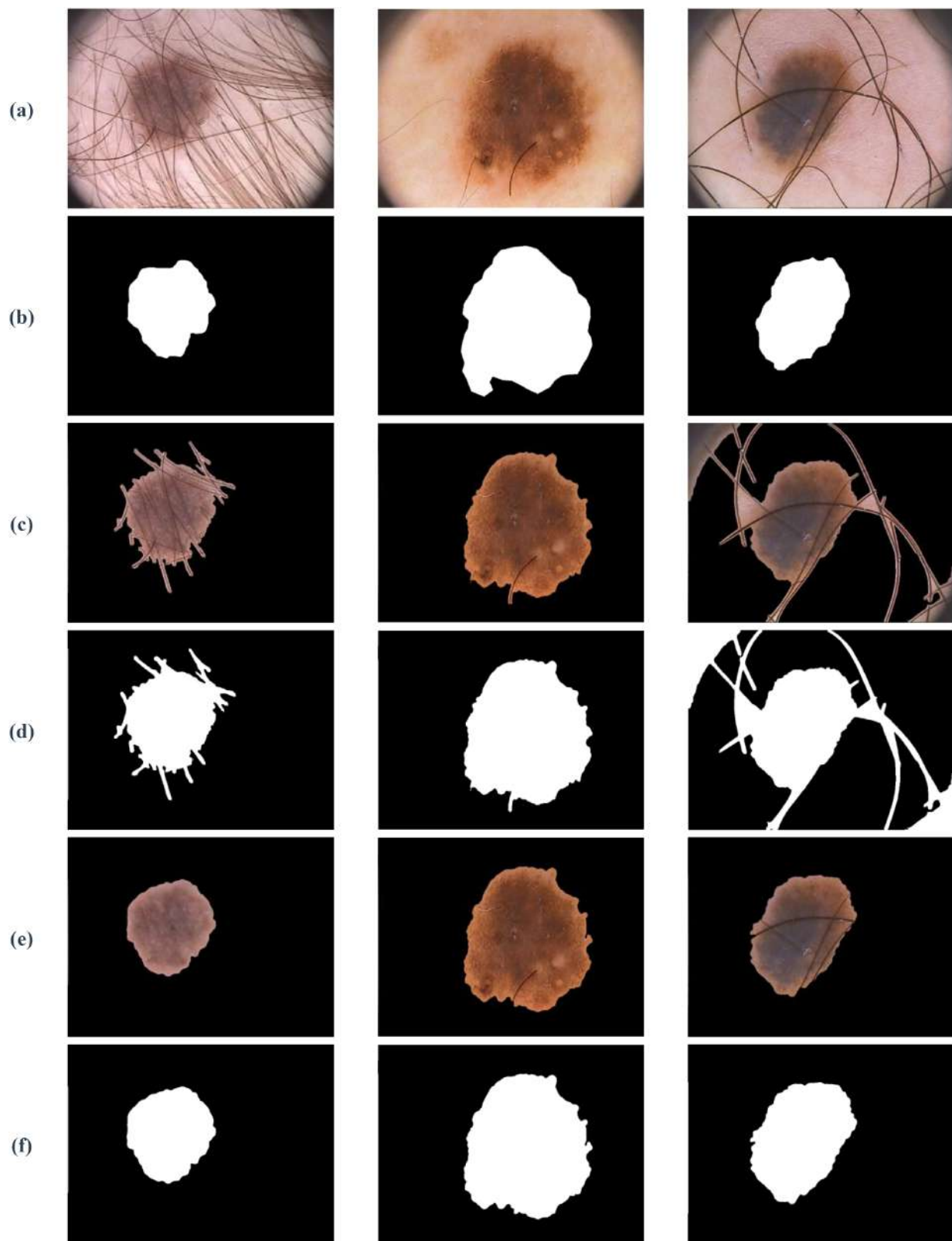


Fig. 4. Segmentation results with (WP) and without (WOP) pre-processing: (a) original image, (b) ground truth, (c) lesion extraction (WOP), (d) segmented image (WOP), (e) lesion extraction (WP), and (f) segmented image (WP).

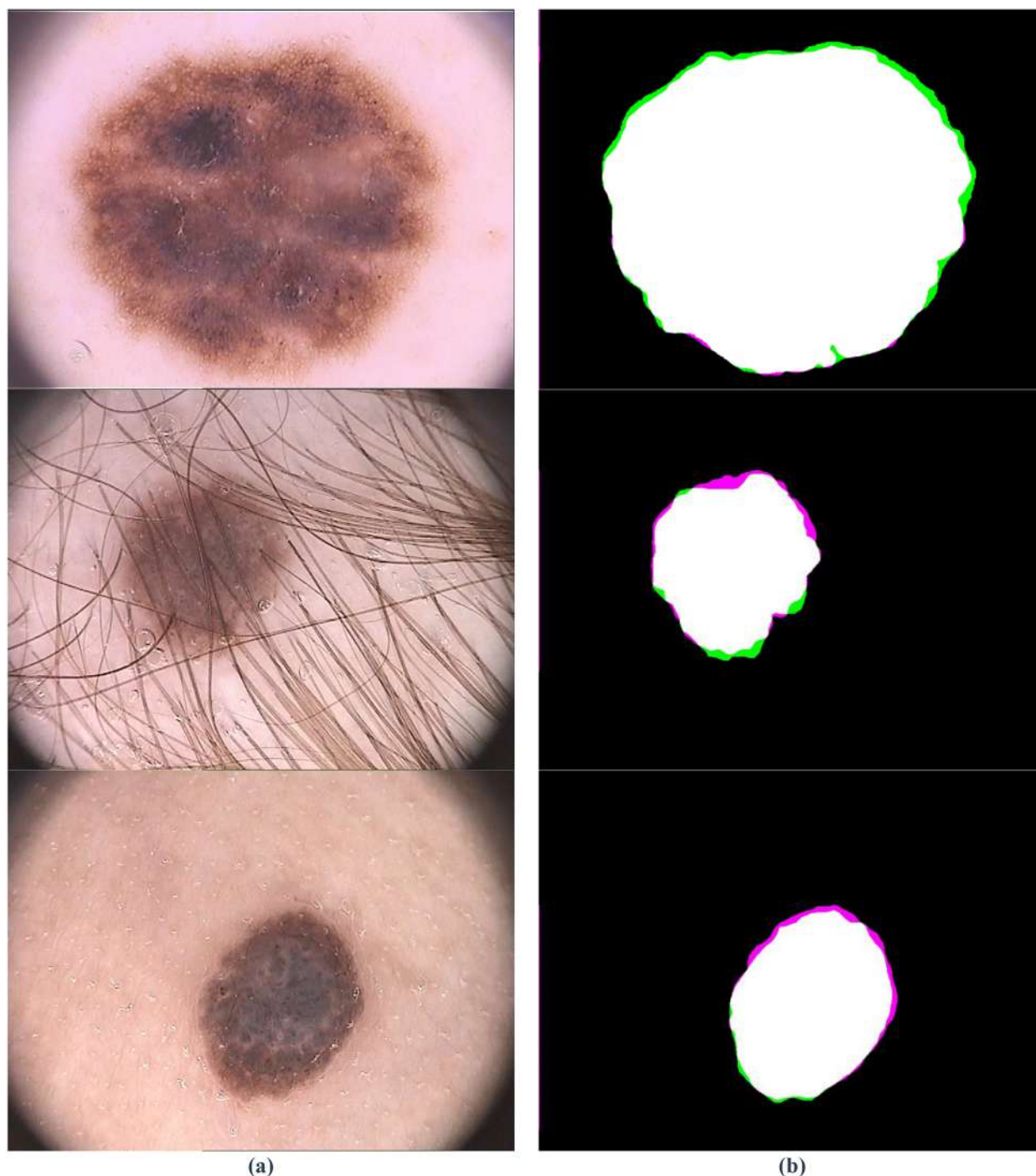


Fig. 5. Visual comparison (a) original image and (b) overlay image. White indicates areas of overlap between the segmented and ground truth images, green indicates true detections, and purple indicates false detections or areas where the segmented image differs from the ground truth.

Comparison with the ground truth

In addition to quantitative metrics, visual comparison can be a valuable way to evaluate the performance of our segmentation algorithm. Visual inspection can provide insights into specific areas of the image where the algorithm is failing, such as areas where the boundaries between different segments are

unclear or where the segmentation is not accurately capturing essential features of the image. See Fig. 5.

Comparison with the SOTA methods

In order to assess the resilience of our proposed method, the authors used the PH2 dataset for the

Table 5. Quantitative measurements of our proposed segmentation method and SOTA methods.

Method	Year	Acc (%)	Pre (%)	Sen (%)	Spe (%)	JI (%)	D (%)
Goyal et al. ¹⁹	2019	93.80	–	93.20	92.90	83.90	90.70
Pereira et al. ⁶	2020	–	–	–	–	86.30	–
Öztürk and Özkaya ⁷	2020	96.92	–	–	–	87.10	93.02
Abhishek et al. ²⁰	2020	89.26	–	84.42	96.07	75.59	85.37
Xie et al. ²¹	2020	94.90	–	96.30	94.20	85.70	91.90
Ramya et al. ²²	2021	86.93	91.38	90.40	–	–	88.40
Araújo et al. ²³	2022	–	–	–	–	–	92.30
Chen et al. ²⁴	2022	95.14	–	89.23	96.75	86.15	92.12
Rehman et al. ¹³	2022	–	–	–	–	77.00	87.00
Zafar et al. ²⁵	2023	95.91	–	–	–	–	–
Wang et al. ²⁶	2023	94.10	–	95.80	94.20	87.70	93.50
Proposed method	2024	96.14	93.87	94.49	95.99	88.19	94.21

proposed segmentation method because it contains the ground truth for each image. In contrast, use the Skin_Hair dataset, which includes artificial hair generated with its corresponding ground truth. On the other hand, some PH2 dataset images have hair artifacts that the proposed pre-processing method can remove. As a result, our proposed approaches exhibited strong performances, surpassing various other impressive models. Table 5 comprehensively compares our proposed segmentation method and several SOTA models.

Table 5 shows that our proposed method outperformed the other methods, achieving an Acc of 96.14% and a Pre of 93.87%. Additionally, our method showed a high Sen of 94.49% and a high Spe of 95.99%, indicating its ability to identify positive and negative cases correctly. The JI and D measures of 88.19% and 94.21%, respectively, further demonstrate the effectiveness of our proposed method. These results suggest that our method could be valuable for skin imaging analysis and diagnosis. However, more research is needed to validate the method on larger datasets and to assess its clinical feasibility.

Conclusion

Detecting skin cancer is a vital process that requires the examination of skin lesions through dermoscopy images. However, image segmentation is a challenging step in this process that requires integrating various features. However, to tackle this problem, our research proposed a novel approach for skin dermoscopy image segmentation using histogram feature fusion. Additionally, the authors developed a methodology for removing artifacts and digital hair from skin dermoscopy images using photometric quasi-invariants. Our proposed skin dermoscopy segmentation method involves extracting the histogram's data range and mean images and then fusing them to create a final image. The fused image significantly helps in the segmentation process, which

is crucial for detecting skin cancer accurately. The authors used the PH2 dataset for the proposed segmentation method because it contains the ground truth for each image. In contrast, use the Skin_Hair dataset, which includes artificial hair generated with its corresponding ground truth.

On the other hand, some PH2 dataset images have hair artifacts that the proposed pre-processing method can remove. Our method's results surpassed SOTA accuracy, efficiency, and robust approaches. Specifically, the proposed approach achieved an average Acc 96.14, Pre 93.87, Sen 94.49, Spe 95.99, JI 88.19, and D 94.21. These results demonstrate the superiority of our proposed approach over the existing SOTA approaches regarding Pre, D, and JI metrics. Our research proposes a novel approach for skin dermoscopy image segmentation using histogram feature fusion, an essential step in accurately detecting skin cancer. Therefore, it has the potential to assist dermatologists and healthcare professionals in making more accurate and timely diagnoses of skin cancer. Also, the proposed approach showed robustness to variations in image quality and lesion appearance, which are common challenges in skin lesion segmentation. One key limitation is the computational complexity of the proposed approach, particularly in processing high-resolution images. One future work for skin lesion segmentation using the proposed method could be applied to more diverse datasets. Applying the proposed method to a more diverse dataset can be validated if the model also performs well on different skin lesions and conditions.

Authors' declaration

- Conflicts of Interest: None.
- We hereby confirm that all the Figures and Tables in the manuscript are ours. Furthermore, any Figures and images that are not ours have been included with the necessary permission for republication, which is attached to the manuscript.

- No animal studies are present in the manuscript.
- Author(s) signed off on ethical considerations' approval.
- Ethical Clearance: The project was approved by the local ethical committee at Universiti Teknologi Malaysia.

Authors' contribution statement

F. H. N. contributed to the conceptualization, methodology, and initial drafting of the manuscript. F. M., as the supervisor, guided the research project, contributed to the study design. A. N. H. assisted in data collection, analysis, interpretation, and the writing and editing of the manuscript. M. S. M. provided expert advice on research design and methodology, reviewed the manuscript. K. A. K. participated in data analysis and visualization, contributed to the literature review.

Data availability

The datasets generated and analyzed during the current study are available in the Skin_Hair dataset, <https://skin-hairdataset.github.io/SHD/> and PH2 datasets <https://www.fc.up.pt/addi/ph2%20database.html>.

References

- Dobre EG, Surcel M, Constantin C, Ilie MA, Caruntu A, Caruntu C, *et al.* Skin cancer pathobiology at a glance: a focus on imaging techniques and their potential for improved diagnosis and surveillance in clinical cohorts. *Int J Mol Sci.* 2023 Jan 5;24(2):1–58. <https://doi.org/10.3390/ijms24021079>.
- Liu L, Mou L, Zhu XX, Mandal M. Automatic skin lesion classification based on mid-level feature learning. *Comput Med Imaging Graph.* 2020 1;84:101765. <https://doi.org/10.1016/j.compmedimag.2020.101765>.
- Singh L, Janghel RR, Sahu SP. Designing a retrieval-based diagnostic aid using effective features to classify skin lesion in dermoscopic images. *Procedia Comput Sci* 2020 Jan 1;167:2172–80. <https://doi.org/10.1016/j.procs.2020.03.267>.
- Varma PB, Paturu S, Mishra S, Rao BS, Kumar PM, Krishna NV. SLDCNet: Skin lesion detection and classification using full resolution convolutional network-based deep learning CNN with transfer learning. *Expert Syst.* 2022 Nov;39(9):12944. <https://doi.org/10.1111/exsy.12944>.
- Zafar K, Gilani SO, Waris A, Ahmed A, Jamil M, Khan MN, *et al.* Skin lesion segmentation from dermoscopic images using convolutional neural network. *Sensors.* 2020 Mar 13;20(6):1601. <https://doi.org/10.3390/s20061601>.
- Pereira PM, Fonseca-Pinto R, Paiva RP, Assuncao PA, Tavora LM, Thomaz LA, *et al.* Dermoscopic skin lesion image segmentation based on Local Binary Pattern Clustering: Comparative study. *Biomed Signal Process Control.* 2020 May 1;59:101924. <https://doi.org/10.1016/j.bspc.2020.101924>.
- Öztürk Ş, Özkaya U. Skin lesion segmentation with improved convolutional neural network. *J Digit Imaging.* 2020;33:958–70. <https://doi.org/10.1007/s10278-020-00343-z>.
- Qin Z, Liu Z, Zhu P, Xue Y. A GAN-based image synthesis method for skin lesion classification. *Comput Methods Programs Biomed.* 2020 Oct 1;195:105568. <https://doi.org/10.1016/j.cmpb.2020.105568>.
- Li Z, Koban KC, Schenck TL, Giunta RE, Li Q, Sun Y. Artificial intelligence in dermatology image analysis: current developments and future trends. *J Clin Med.* 2022 Nov 18;11(22):6826. <https://doi.org/10.3390/jcm11226826>.
- Kaur C, Garg U. Artificial intelligence techniques for cancer detection in medical image processing: A review. *Mater Today: Proceedings.* 2023 Jan 1;81:806–9. <https://doi.org/10.1016/j.matpr.2021.04.241>.
- Zhang Z, Ye S, Liu Z, Wang H, Ding W. Deep hyperspherical clustering for skin lesion medical image segmentation. *IEEE J Biomed Health Inform.* 2023 Jan 27;27(8):3770–81. <https://doi.org/10.1109/JBHI.2023.3240297>.
- Barin S, Güraksın GE. An automatic skin lesion segmentation system with hybrid FCN-ResAlexNet. *Eng Sci. Technol Int J.* 2022 Oct 1;34:101174. <https://doi.org/10.1016/j.jestch.2022.101174>.
- Rehman M, Ali M, Obayya M, Asghar J, Hussain L, K Nour M, *et al.* Machine learning based skin lesion segmentation method with novel borders and hair removal techniques. *Plos one.* 2022 Nov 10;17(11):e0275781. <https://doi.org/10.1371/journal.pone.0275781>.
- Ahammed M, Al Mamun M, Uddin MS. A machine learning approach for skin disease detection and classification using image segmentation. *Healthc Anal.* 2022 Nov 1;2:100122. <https://doi.org/10.1016/j.health.2022.100122>.
- Jaworek-Korjakowska J, Wojcicka A, Kucharski D, Brodzicki A, Kendrick C, Cassidy B, *et al.* Skin_Hair dataset: Setting the benchmark for effective hair inpainting methods for improving the image quality of dermoscopic images. *European Conference on Computer Vision: Springer Nature Switzerland;* 2022 Oct.:167–184. https://doi.org/10.1007/978-3-031-25069-9_12.
- Alenezi F, Armghan A, Polat K. A multi-stage melanoma recognition framework with deep residual neural network and hyperparameter optimization-based decision support in dermoscopy images. *Expert Syst Appl.* 2023 Apr 1;215:119352. <https://doi.org/10.1016/j.eswa.2022.119352>.
- Li W, Raj AN, Tjahjadi T, Zhuang Z. Digital hair removal by deep learning for skin lesion segmentation. *Pattern Recognit.* 2021 Sep 1;117:107994. <https://doi.org/10.1016/j.patcog.2021.107994>.
- Attia M, Hossny M, Zhou H, Nahavandi S, Asadi H, Yazdabadi A. Realistic hair simulator for skin lesion images: A novel benchmarking tool. *Artif Intell Med.* 2020 Aug 1;108:101933. <https://doi.org/10.1016/j.artmed.2020.101933>.
- Goyal M, Oakley A, Bansal P, Dancey D, Yap MH. Skin lesion segmentation in dermoscopic images with ensemble deep learning methods. *IEEE Access.* 2019 Dec 18;8:4171–81. <https://doi.org/10.1109/ACCESS.2019.2960504>.
- Kumar A, Hamarneh G, Drew MS. Illumination-based Transformations Improve Skin Lesion Segmentation in Dermoscopic Images. *IEEE/CVF Conference on Computer Vision and Pattern Recognition Workshops (CVPRW).* 2020 Jun 1:3132–3141. *IEEE Computer Society.* <https://doi.org/10.1109/CVPRW50498.2020.00372>.
- Xie F, Yang J, Liu J, Jiang Z, Zheng Y, Wang Y. Skin lesion segmentation using high-resolution convolutional neural network. *Comput Methods Programs Biomed.* 2020 Apr 1;186:105241. <https://doi.org/10.1016/j.cmpb.2019.105241>.

22. Ramya J, Vijayalakshmi HC, Saifuddin HM. Segmentation of skin lesion images using discrete wavelet transform. *Biomed Signal Process Control*. 2021 Aug 1;69:102839. <https://doi.org/10.1016/j.bspc.2021.102839>.
23. Araújo RL, Araújo FH, Silva RR. Automatic segmentation of melanoma skin cancer using transfer learning and fine-tuning. *Multimed Syst.* 2022 Aug;28(4):1239–50. <https://doi.org/10.1007/s00530-021-00840-3>.
24. Chen P, Huang S, Yue Q. Skin lesion segmentation using recurrent attentional convolutional networks. *IEEE Access*. 2022 Sep 5;10:94007–18. <https://doi.org/10.1109/ACCESS.2022.3204280>.
25. Zafar M, Amin J, Sharif M, Anjum MA, Mallah GA, Kadry S. DeepLabv3+ -based segmentation and best features selection using slime mould algorithm for multi-class skin lesion classification. *Mathematics*. 2023 Jan 10;11(2):364. <https://doi.org/10.3390/math11020364>.
26. Wang J, Tang Y, Xiao Y, Zhou JT, Fang Z, Yang F. GREnet: gradually recurrent network with curriculum learning for 2-D medical image segmentation. *IEEE Trans Neural Netw Learn Syst*. 2023 Jan 26. <https://doi.org/10.1109/TNNLS.2023.3238381>.
27. Najjar FH, Khudhair KT, Khaleq AH, Kadhim ON, Abedi F, Al-Kharsan IH. Histogram features extraction for edge detection approach. *5th International Conference on Engineering Technology and its Applications (IICETA)*. 2022 May 31: 373–378. IEEE. <https://doi.org/10.1109/IICETA54559.2022.9888697>.
28. Mendonça T, Ferreira PM, Marques JS, Marcal AR, Rozeira J. PH 2-A dermoscopic image database for research and benchmarking. *35th annual international conference of the IEEE engineering in medicine and biology society (EMBC)*. IEEE; 2013 Jul 3:5437–5440. <https://doi.org/10.1109/EMBC.2013.6610779>.

تجزئة دقيقة للآفات الجلدية من خلال دمج الميزات في صور سرطان الجلد

فلاح حسن نجار^{1،2}، فرحان محمد¹، اسينياني نور حيدر^{1،3}، محمد شفري محمد رحيم¹، كرار عبد الأمير كاظم^{1،4}

¹ قسم الحوسبة الناشئة، كلية الحاسبات، الجامعة التكنولوجية الماليزية، جوهور باهرو، ماليزيا.

² قسم تقنيات شبكات وبرامجيات الحاسوب، المعهد التقني النجف، جامعة الفرات الأوسط التقنية، النجف، العراق.

³ كلية تكنولوجيا المعلومات والاتصالات، جامعة التقنية الماليزية ملقا، ملقا، ماليزيا.

⁴ قسم هندسة تقنيات الحاسوب، كلية تكنولوجيا المعلومات، جامعة الامام جعفر الصادق، بغداد، العراق.

المستخلص

يتضمن تشخيص سرطان الجلد غالبًا تحليل dermoscopy images لآفات الجلد، والتي تتطلب تقنيات تجزئة الصور لاستخراج الميزات ذات الصلة. تقترح أبحاثنا منهجية جديدة لتحسين دقة تجزئة صور (dermoscopy) للجلد عن طريق إزالة الشوائب والشعر باستخدام (photometric quasi-invariants)، يليها نهج جديد لتجزئة الآفات الجلدية باستخدام (histogram feature fusion)، والذي يتضمن استخراج (data range) وصور (mean) من المدرج التكراري ودمجها مع الصورة الخالية من الشوائب والشعر لغرض توليد الصورة النهائية. تم إجراء تجاربنا الخاصة بالمعالجة المسبقة والتجزئة على مجموعتي بيانات (Skin_Hair) و (PH2). أظهرت النتائج التجريبية أن طريقتنا حققت دقة وكفاءة وقوة أعلى من الأساليب الحالية، كما تم قياسها بدقة (Accuracy (Acc)، و (Precision (Pre)، و Sensitivity (Sen)، و Specificity (Spe)، و Jaccard Index (JI)، و Dice (D). حققت طريقتنا المقترحة متوسط Acc 96.14، Sen 94.49، Spe 95.99، JI 88.19، Pre 93.87، و D 94.21. تشير هذه النتائج إلى أن منهجيتنا يمكن أن توفر طريقة أكثر فعالية ودقة لاكتشاف سرطان الجلد.

الكلمات المفتاحية: إزالة الشوائب والشعر، dermoscopic، دمج الميزات، التجزئة، سرطان الجلد.